# Angles-Only Navigation: Position and Velocity Solution from Absolute Triangulation

GEORGE H. KAPLAN

U.S. Naval Observatory, Washington DC, 20392*

ABSTRACT: *Angles-only (or bearings-only) navigation involves determining position, velocity, or orientation information for an observer using the apparent directions or motions of objects at finite distances. Angles-only navigation covers a broad range of applications, and is generally implemented through a Kalman filter that uses imaging and other information to differentially adjust the values of the navigation parameters (state vector) at each incremental step of the observer's computed motion.*

*This paper presents an algorithm for angles-only navigation that is a closed-form solution for both position and velocity that does not require any prior estimate of the observer's position or motion. It is least-squares-based triangulation generalized to a moving observer, involving only angular observations of objects with known coordinates.*

*The algorithm can be applied to any situation where foreground objects are observed against background objects, so long as both foreground and background objects are identifiable and have known coordinates. It can be used for ship piloting using images of shore objects at various distances. It also has possible applications in robotics; for example, for determining the position and velocity of mobile landers on other solar system bodies, or for automated farming. A specific proposed application for open-sea ship navigation would use the angular positions of Earth satellites observed optically against a star background. Such a system could provide a supplement to ordinary GPS navigation, as well as supplying a precise absolute attitude reference.*

## INTRODUCTION

This paper outlines the geometry and corresponding mathematics of a particular type of angles-only navigation. In angles-only navigation (also known as bearings-only navigation) position, velocity, or orientation information for an observer is passively obtained from measurements of the apparent angles, or angular rates, of objects at finite (but generally unknown) distances. Despite its name, angles-only navigation is often used to augment other means of navigation, such as dead reckoning, inertial, or GPS. As a simple example, a ship's navigator can determine a line of position from the measured bearing of an identifiable navigation aid or landmark. Two such lines of position will cross at the ship's position. In more sophisticated forms, it has been applied to spacecraft maneuvering [1, 2], aircraft navigation [3–6], and position determination for mobile robots [7–9]. Advances in electronic imaging and real-time image analysis capabilities over the last few decades have considerably expanded the scope of uses, and the literature base has blossomed, with significant contributions from fields such as optics, computer vision, robotics, artificial intelligence, and even animal navigation. The topic is probably too broad for a review even to be possible, and the references cited above are just a tiny sample of the papers published.

In the most common implementations of angles-only navigation, measurements from a scene recorded by an imaging system serve as input, along with data from other sensors, to a navigational Kalman filter that continually updates the observer's state vector (e.g, position, velocity, and attitude); see, for example, [10]. For this purpose, the sensitivity of the scene elements and other sensor data to a change of state are linearized about an estimated state, which is a computational projection based on previous data. The differences between the measurements and their expected values, which are assumed small, provide information to correct the estimated state, and the cycle repeats. A somewhat different kind of predictive stepwise filter for angles-only measurements, yielding position, velocity, attitude, and rotation, was published in [11].

In this paper, however, we consider how to determine, *ab initio*, both the position and velocity

| Report Documentation Page | | *Form Approved* *OMB No. 0704-0188* |
|---|---|---|

| 1. REPORT DATE **JUL 2010** | 2. REPORT TYPE | 3. DATES COVERED **00-00-2010 to 00-00-2010** |
|---|---|---|
| 4. TITLE AND SUBTITLE **Angels-Only Navigation: Position And Velocity Solution From Absolute Triangulation** | | 5a. CONTRACT NUMBER |
| | | 5b. GRANT NUMBER |
| | | 5c. PROGRAM ELEMENT NUMBER |
| 6. AUTHOR(S) | | 5d. PROJECT NUMBER |
| | | 5e. TASK NUMBER |
| | | 5f. WORK UNIT NUMBER |
| 7. PERFORMING ORGANIZATION NAME(S) AND ADDRESS(ES) **U. S. Naval Observatory,Washington,DC,20392** | | 8. PERFORMING ORGANIZATION REPORT NUMBER |
| 9. SPONSORING/MONITORING AGENCY NAME(S) AND ADDRESS(ES) | | 10. SPONSOR/MONITOR'S ACRONYM(S) |
| | | 11. SPONSOR/MONITOR'S REPORT NUMBER(S) |

| 12. DISTRIBUTION/AVAILABILITY STATEMENT |
|---|
| **Approved for public release; distribution unlimited** |

| 13. SUPPLEMENTARY NOTES |
|---|
| **Navigation, Journal of the Institute of Navigation,v. 58, no. 3, Fall 2011** |

14. ABSTRACT

**Angles-only (or bearings-only) navigation involves determining position, velocity, or orientation information for an observer using the apparent directions or motions of objects at finite distances. Angles-only navigation covers a broad range of applications, and is generally implemented through a Kalman filter that uses imaging and other information to differentially adjust the values of the navigation parameters (state vector) at each incremental step of the observer's computed motion. This paper presents an algorithm for angles-only navigation that is a closed-form solution for both position and velocity that does not require any prior estimate of the observer's position or motion. It is least-squares-based triangulation generalized to a moving observer, involving only angular observations of objects with known coordinates. The algorithm can be applied to any situation where foreground objects are observed against background objects, so long as both foreground and background objects are identifiable and have known coordinates. It can be used for ship piloting using images of shore objects at various distances. It also has possible applications in robotics; for example, for determining the position and velocity of mobile landers on other solar system bodies, or for automated farming. A specific proposed application for open-sea ship navigation would use the angular positions of Earth satellites observed optically against a star background. Such a system could provide a supplement to ordinary GPS navigation, as well as supplying a precise absolute attitude reference.**

| 15. SUBJECT TERMS | | | | | |
|---|---|---|---|---|---|
| 16. SECURITY CLASSIFICATION OF: | | | 17. LIMITATION OF ABSTRACT | 18. NUMBER OF PAGES | 19a. NAME OF RESPONSIBLE PERSON |
| a. REPORT **unclassified** | b. ABSTRACT **unclassified** | c. THIS PAGE **unclassified** | **Same as Report (SAR)** | **9** | |

vectors of an observer (e.g., an imaging system) using a sequence of angular measurements that are distributed over a period of time. The measurements are of the apparent directions of identifiable objects with known coordinates. The scheme is "absolute" in the sense that the angular measurements, rather than being relative to some unknown directions, are expressed in the reference system that is used for the object coordinates (and the navigation solution). This considerably simplifies the problem by obviating the need for a simultaneous attitude solution or any kind of object-space/image-space mapping. Although at first thought this situation may seem atypical, the development remains pertinent to many common applications. For example, it is relevant to any system that captures scenes in which foreground features appear against background features, and geodetic coordinates can be obtained for both near and far objects.

In contrast to the Kalman filter approach, the algorithm presented here does not require any previous estimate of position or motion, and is of closed form, not stepwise or iterative. It is a type of 3-D triangulation applied to a moving observer, with angular observations taken at various positions along the observer's track. The observations are assumed to be uncorrelated and to have normally distributed random errors but no significant systematic errors. The solution minimizes the effects of errors in both the observations and the assumed object coordinates in a least-squares sense. Since the algorithm requires only information related to the angular observations, it may be useful for startup situations or any other circumstances in which current position and velocity data are unreliable or not available. The scheme requires only that the objects observed can be identified and their coordinates retrieved. The algorithm can also provide a check on stepwise navigation filters. The development is based on a straightforward geometric construction and the solutions are robust for reasonable sets of observations.

What is presented here is not, of course, the first closed-form solution to an angles-only navigation problem. In fact, the solution for the fixed-observer case was published (in a different kind of notation) in an appendix to the classical text *Geodesy* by Bomford [12]. Two of the robotics papers mentioned above [7, 9] present closed-form solutions for a fixed observer using relative bearing measurements in a 2-D environment. The main contribution of this paper is in presenting a closed-form solution for both position and velocity in a 3-D environment. The development includes a correction term for the curvature of the Earth, so that observations can be collected over extended tracks.

The paper is organized by sections as follows. First, some possible applications of the method are described. The following section explains the basic concepts of the observations and their representation as vectors. Next, two navigation solutions are presented, one for a fixed observer and the other for a moving observer. The term in the solution that corrects for the curvature of the Earth is then briefly discussed. The next two sections consider the propagation of random error and the effects of an unmodeled acceleration on the solution. The specific possibility of using Earth satellites observed optically (or in the near-infrared) against background stars as the source of observations for this method is described in some detail. The results of a numerical simulation of such an observing system are presented and, finally, the salient points of the paper are summarized.

## APPLICATIONS

The method described in this paper was developed for a proposed shipboard automated celestial observing system that would augment GPS with absolute orientation information and serve as a standalone positioning system in case of GPS denial. The chosen observing mode involved artificial Earth satellites observed optically or in a near-infrared band against background stars. The algorithm described here was initially developed simply to provide quick estimates of the likely errors of such a system, under various conditions, even though the eventual navigation solution was to be obtained from a Kalman filter involving multiple sensor inputs. However, the method has value in itself by providing a standalone navigation solution from the satellite observations in the absence of any other information. The obvious next question was whether the algorithm might be applied in other contexts.

As it turns out, the mathematics provided here could be applied to any situation in which the directions to identifiable objects can be measured with respect to more distant objects, so long as the coordinates of both foreground and background objects are known. When a foreground and a background object appear to line up from the point of view of the observer, the observed direction vector is simply the normalized difference of the position vectors of the two objects. Since the direction vector is computed from absolute coordinates — that is, coordinates relative to a well-defined reference system, such as WGS-84 — it, too, is absolute. Using that type of observation, the algorithm therefore has wide application to any kind of vehicle that has an imaging system, even if not of the highest quality. The accuracy depends only on the resolution of the image, not on any external angular calibration or the transformation of real space to image space.
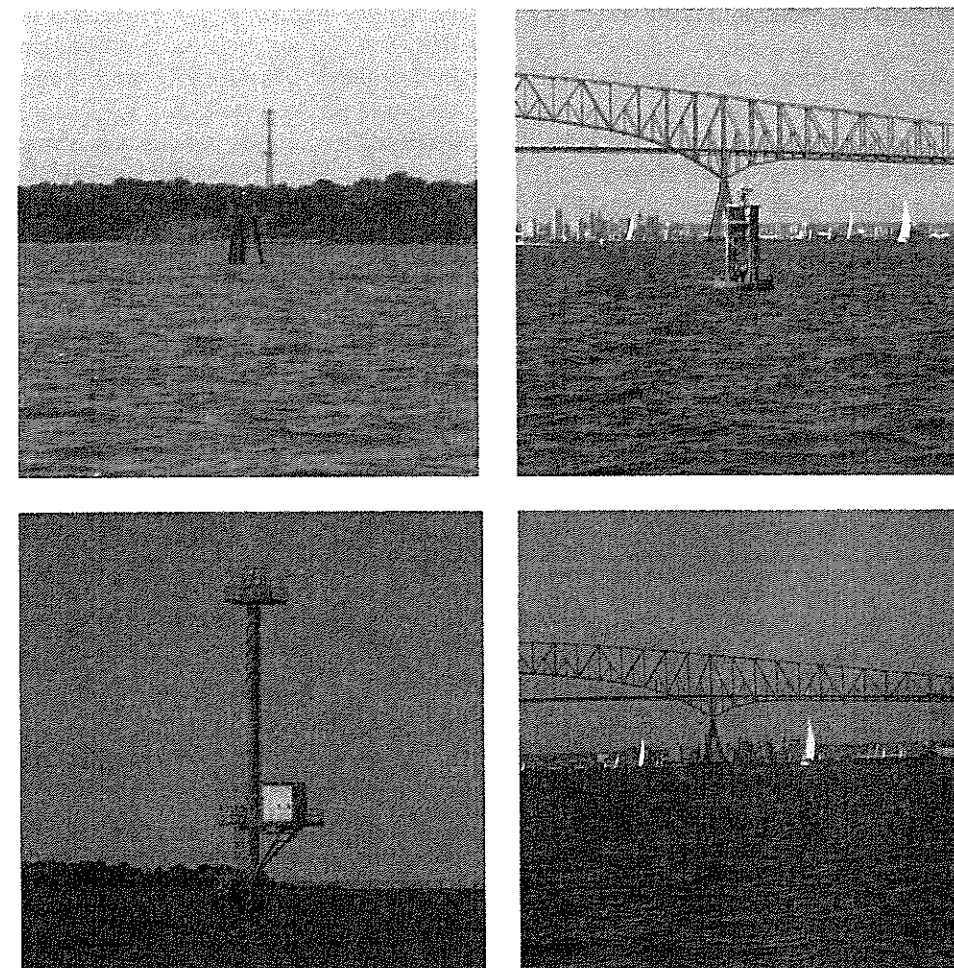


Fig. 1–Images of aligned foreground and background objects viewed from the Patapsco River outside Baltimore. Each image yields a direction vector (line of position) in the WGS-84 system, based on the coordinates of the two objects.

For objects seen near the horizontal plane, the apparent alignment of objects in the vertical direction suffices if the height of the observer is not of interest (i.e., if the 3-D problem effectively collapses to 2-D). For example, as seen from a ship, a buoy may appear to pass underneath a distant water tower. A series of time-tagged images of aligned objects, for which the latitudes and longitudes are known, would allow for a solution for the surface track of the vehicle. The method could be applied to ordinary ship piloting, which was demonstrated by the author using images of shore objects taken during a small-boat trip up the Chesapeake Bay and into Baltimore Harbor (see Figure 1 for examples). The images were taken with an inexpensive hand-held camera and timed only to the nearest minute using the camera's internal clock. For each image, coordinates of the foreground and background objects were subsequently obtained from Google Earth or the USCG Light List [13], and the coordinates converted to geocentric position vectors. Using two vectors derived from each such observation (see next section), a solution for a portion of the boat's track was then computed using the method described in this paper. Despite the primitive nature of the experiment, the solution was close to that obtained from a straight-line fit of the recorded GPS positions of the boat, and the residual errors in both cases (748 and 629 m RMS, respectively) were largely the result of the boat's deviations from the modeled tracks — an important consideration in the practical applicability of the method that will be discussed later. This rudimentary exercise showed, however, that the method might be useful for piloting in areas that are well mapped, or for which good satellite imagery is available, but lack reliable navigational aids. Practical use of the method would require an automated system of object identification that would permit the retrieval of their coordinates from a suitable database.

The method would also apparently work well for navigating robotic landers across the surfaces of other solar system bodies using the on-board imaging system. All that is needed is a database of identifiable
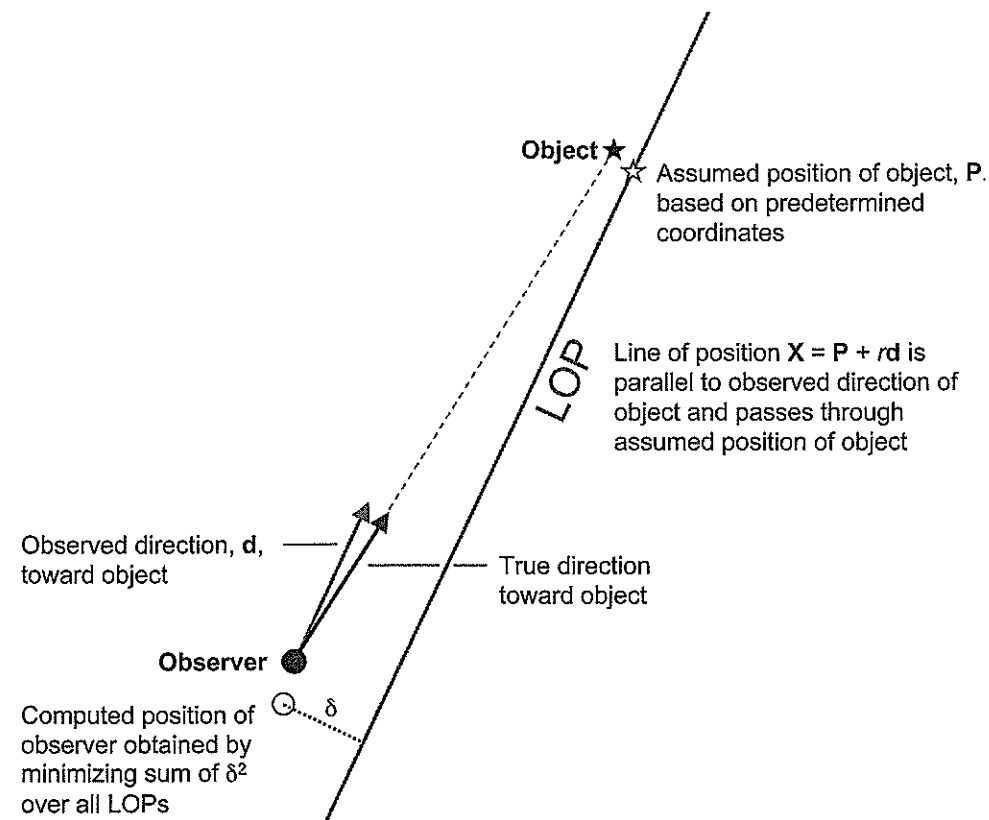
**Object ★**

Assumed position of object, **P**, based on predetermined coordinates

Line of position **X = P + r d** is parallel to observed direction of object and passes through assumed position of object

*LOP*

Observed direction, **d**, toward object

True direction toward object

**Observer**

Computed position of observer obtained by minimizing sum of $\delta^2$ over all LOPs

Fig. 2—*Geometry of a single observation. Both the observed direction of the object and the object's coordinates are assumed to have some error.*

terrain features and their coordinates. In fact, it could be applied to interplanetary space navigation (although not at high accuracy) if the apparent directions of several relatively nearby solar system objects were observed against the star background. Navigation of automated farming systems is another possibility. For example, a system of marked poles at a field's edge, at two different perimeters, might be imaged by a rotating camera on top of a robotic tractor.

## OBSERVATIONS, VECTORS, COORDINATE SYSTEMS

This paper uses the convention that vectors of arbitrary length are written as boldface upper-case letters and unit vectors are written as boldface lower-case letters. For example, **z** would be the unit vector in the direction of **Z**.

The algorithm in this paper is based on observations of the directions of identifiable objects, with known coordinates, from the point of view of an observer whose own coordinates are to be determined. For each object observed, then, two kinds of information are required: the predetermined coordinates of the object, represented by the position vector **P**; and the observation itself, represented by the direction (unit) vector **d**. In the absence of errors, the

observer must be somewhere on a line of position (LOP) in 3-D space given by the equation **X = P + r d**, where **X** is the position of an arbitrary point along the line and $r$ is a scalar that can take on any real value. The components of the vectors **X** and **P** and the scalar $r$ have units of length, while **d** is dimensionless. We assume that **X**, **P**, and **d** may be functions of time; for a moving target, the time series of vectors **P**($t$) is referred to as its ephemeris. See Figure 2.

We require that **P** and **d** are given in, or reduced to, a common coordinate system. For some kinds of observations, this will come about naturally. For example, if a target object is observed against a background object, and both have coordinates in the same database, then the direction vector is simply the difference between the known position vectors of the background object and the target, normalized to unit length. The direction vector is thereby expressed in the coordinate system used for the positions of all the landmarks. A more complicated case is that of artificial Earth satellites imaged against the star background, in which the observations and object coordinates are naturally expressed in different kinds of coordinates and must be reduced to a common system. This is discussed more fully in the section on using satellites as target objects.

The navigation solution vectors will be expressed in the coordinate system used for the object coordinates and observations. Effectively, the set of assumed coordinates for all the objects observed define the reference system for the solution. Since the solution is based on geometry, not dynamics, there is no requirement that the reference system be inertial. In the most common case, in fact, the reference system will be geodetic (Earth-fixed) and therefore not inertial.

## NAVIGATION SOLUTION

We will start with an observer that is fixed with respect to the objects he is observing, at location **X**. Given an ensemble of $n$ observations $\mathbf{d}_i$ of objects at known positions $\mathbf{P}_i$, respectively, the least-squares estimate for **X** is given by

$$
\begin{pmatrix} n - [d_{i_1}^2] & -[d_{i_1}d_{i_2}] & -[d_{i_1}d_{i_3}] \\ -[d_{i_1}d_{i_2}] & n - [d_{i_2}^2] & -[d_{i_2}d_{i_3}] \\ -[d_{i_1}d_{i_3}] & -[d_{i_2}d_{i_3}] & n - [d_{i_3}^2] \end{pmatrix} \begin{pmatrix} x_1 \\ x_2 \\ x_3 \end{pmatrix}
$$

$$
= \begin{pmatrix} [P_{i_1} - (\mathbf{d}_i \cdot \mathbf{P}_i)d_{i_1}] \\ [P_{i_2} - (\mathbf{d}_i \cdot \mathbf{P}_i)d_{i_2}] \\ [P_{i_3} - (\mathbf{d}_i \cdot \mathbf{P}_i)d_{i_3}] \end{pmatrix} \qquad (1)
$$

where $\mathbf{P}_i = (P_{i_1}, P_{i_2}, P_{i_3})$, $\mathbf{d}_i = (d_{i_1}, d_{i_2}, d_{i_3})$, $\mathbf{X} = (x_1, x_2, x_3)$, and the square brackets indicate a summation over all $n$ observations, i.e., $[\ldots]$ represents $\sum_{i=1}^{n} \ldots$.

This is a system of three scalar equations in three unknowns, $x_1$, $x_2$, and $x_3$, the components of the observer's position vector. These three equations are equivalent to Equation (C.29) in [12]. We have minimized the sum $\mathcal{D} = \sum_i \delta_i^2$, where each $\delta_i$ represents the distance of line of position $i$, defined by the observation $i$, from **X**, the computed position of the observer. We imagine all of the LOPs converging in a small volume of 3-D space; **X** is in the center of this volume, with "center" precisely defined by the least-squares criterion.

There is a brute-force solution to Equation (1) from substitution. If we re-cast (1) as

$$
\begin{pmatrix} A & B & C \\ B & D & E \\ C & E & F \end{pmatrix} \begin{pmatrix} x_1 \\ x_2 \\ x_3 \end{pmatrix} = \begin{pmatrix} Q_1 \\ Q_2 \\ Q_3 \end{pmatrix}
$$

with $A = n - [d_{i_1}^2]$, $B = -[d_{i_1}d_{i_2}]$, etc., then the solution is

$$
x_3 = \frac{(CD - BE)(CQ_1 - AQ_3) - (BC - AE)(CQ_2 - BQ_3)}{(CD - BE)(C^2 - AF) - (BC - AE)(CE - BF)}
$$

$$
x_2 = \frac{CQ_2 - BQ_3 - (CE - BF)x_3}{CD - BE}
$$

$$
x_1 = \frac{Q_1 - Bx_2 - Cx_3}{A} \qquad (2)
$$

Because this development applies only to a fixed observer, or $n$ simultaneous observations, it is of limited use for navigation. For simplicity, we have also not considered weighting the observations, although providing for that is straightforward, and is described at the end of this section.

The more useful case is that of a moving observer and non-simultaneous observations. Let us represent the observer's trajectory by $\mathbf{X}(t) = \mathbf{X}(t_0) + \mathbf{V}(t_0)t + f(t)\mathbf{x}_0$, where $\mathbf{X}(t_0)$ and $\mathbf{V}(t_0)$ are the observer's position and velocity, respectively, at time $t_0$. In the third term, $\mathbf{x}_0$ is the unit vector in the direction $\mathbf{X}(t_0)$ and $f(t)$ is a scalar function with units of distance. The time $t$ is measured from the time origin $t_0$, which can be chosen for convenience; it is an arbitrary time that is within or not far outside the span of observation times ($t_1$ to $t_n$) but it does not necessarily correspond to the time of a specific observation. The observations occur at discrete times $t_i$ (measured from $t_0$), and for those times the trajectory can be expressed as $\mathbf{X}_i = \mathbf{X}_0 + \mathbf{V}_0 t_i + f_i \mathbf{x}_0$, using the shorthand $\mathbf{X}_i = \mathbf{X}(t_i)$, $\mathbf{X}_0 = \mathbf{X}(t_0)$, $\mathbf{V}_0 = \mathbf{V}(t_0)$, and $f_i = f(t_i)$.

The third term represents any curvature in the observer's path in the direction $\mathbf{x}_0$, which, if a geocentric coordinate system is used and $f(t) < 0$, is toward the center of the Earth. Thus, the third term could represent the gravitational acceleration of an object in Earth orbit or, for an observer traveling on or near Earth's surface, the local curvature of the geoid. If the third term is written as $f_i \mathbf{X}_0 / X_0$, where $X_0 = |\mathbf{X}_0|$, then $\mathbf{X}_i = \mathbf{X}_0 \left(1 + \frac{f_i}{X_0}\right) + \mathbf{V}_0 t_i$. The curvature term is assumed small compared to the other terms, i.e., that $f_i \ll X_0$ and $f_i \ll |\mathbf{V}_0| \Delta t$, where $\Delta t = |t_n - t_1|$ is the span of time covered by the observations. It is also assumed that $f_i / X_0$ (which is small) can be considered known to sufficient accuracy. The calculation of $f_i$ can be done in a number of ways and is not essential to the method; see next section.

The equation below represents a least-squares solution to the navigation problem; specifically, it minimizes the sum $\mathcal{D} = \sum_i \delta_i^2$ where each $\delta_i$ represents the distance of line of position $i$, defined by the observation taken at time $t_i$, from $\mathbf{X}_i$, the computed position of the observer at the same instant. The geometric interpretation of the solution is similar to that for the fixed-observer case, but less intuitive. The LOPs do not converge to define a small volume of space; rather, they converge around the observer's computed path in such a way that at the time of each observation, the observer is as close as possible to the LOP given the simple model we are adopting for his motion and the fact that the closeness criterion (square of the distance) is assessed in the aggregate for all the LOPs.

The solution algorithm, derived elsewhere [14] is:

$$
\begin{pmatrix}
[(d_{i_1}^2-1)\beta_i^2] & [d_{i_1}d_{i_2}\beta_i^2] & [d_{i_1}d_{i_3}\beta_i^2] & [(d_{i_1}^2-1)t_i\beta_i] & [d_{i_1}d_{i_2}t_i\beta_i] & [d_{i_1}d_{i_3}t_i\beta_i] \\
[d_{i_2}d_{i_1}\beta_i^2] & [(1-d_{i_2}^2)\beta_i^2] & [d_{i_2}d_{i_3}\beta_i^2] & [d_{i_2}d_{i_1}t_i\beta_i] & [(d_{i_2}^2-1)t_i\beta_i] & [d_{i_2}d_{i_3}t_i\beta_i] \\
[d_{i_3}d_{i_1}\beta_i^2] & [d_{i_3}d_{i_2}\beta_i^2] & [(d_{i_3}^2-1)\beta_i^2] & [d_{i_3}d_{i_1}t_i\beta_i] & [d_{i_3}d_{i_2}t_i\beta_i] & [(d_{i_3}^2-1)t_i\beta_i] \\
[(d_{i_1}^2-1)t_i\beta_i] & [d_{i_1}d_{i_2}t_i\beta_i] & [d_{i_1}d_{i_3}t_i\beta_i] & [(d_{i_1}^2-1)t_i^2] & [d_{i_1}d_{i_2}t_i^2] & [d_{i_1}d_{i_3}t_i^2] \\
[d_{i_2}d_{i_1}t_i\beta_i] & [(d_{i_2}^2-1)t_i\beta_i] & [d_{i_2}d_{i_3}t_i\beta_i] & [d_{i_2}d_{i_1}t_i^2] & [(d_{i_2}^2-1)t_i^2] & [d_{i_2}d_{i_3}t_i^2] \\
[d_{i_3}d_{i_1}t_i\beta_i] & [d_{i_3}d_{i_2}t_i\beta_i] & [(d_{i_3}^2-1)t_i\beta_i] & [d_{i_3}d_{i_1}t_i^2] & [d_{i_3}d_{i_2}t_i^2] & [(d_{i_3}^2-1)t_i^2]
\end{pmatrix}
\begin{pmatrix} x_1 \\ x_2 \\ x_3 \\ v_1 \\ v_2 \\ v_3 \end{pmatrix}
$$

$$
=
\begin{pmatrix}
[-(P_{i_1}-(\mathbf{d}_i\cdot\mathbf{P}_i)d_{i_1})\beta_i] \\
[-(P_{i_2}-(\mathbf{d}_i\cdot\mathbf{P}_i)d_{i_2})\beta_i] \\
[-(P_{i_3}-(\mathbf{d}_i\cdot\mathbf{P}_i)d_{i_3})\beta_i] \\
[-(P_{i_1}-(\mathbf{d}_i\cdot\mathbf{P}_i)d_{i_1})t_i] \\
[-(P_{i_2}-(\mathbf{d}_i\cdot\mathbf{P}_i)d_{i_2})t_i] \\
[-(P_{i_3}-(\mathbf{d}_i\cdot\mathbf{P}_i)d_{i_3})t_i]
\end{pmatrix}
\tag{3}
$$

where, again, the square brackets indicate a summation over all $n$ observations, and $\beta_i = \left(1+\frac{f_i}{X_0}\right)$. The column vector on the left side represents the unknown navigation state, $\mathbf{U}$, at time $t_0$: $\mathbf{U} = (\mathbf{X}_0, \mathbf{V}_0) = (x_1, x_2, x_3, v_1, v_2, v_3)$. The remaining notation is the same as for Equation (1). Note that the time $t_i$ of each observation, measured from $t_0$, appears explicitly in some of the terms. The time $t_0$ can be chosen to be at the *end* of the series of observations, so that Equation (3) can provide a near real-time estimate of position and velocity.

Equation (3) is of the form $AU = Q$, where U and Q are column 6-vectors and A is a 6×6 matrix. The solution is $U = A^{-1}Q$, where $A^{-1}$ is the inverse of A and represents the unscaled covariance matrix of the solution.

For straight-line motion (no curvature term), $\beta_i = 1$ for all $i$. Also, if the observer is stationary, then $t_i$ can be considered to be 0 for all $i$ since time is measured from when the observer was at $\mathbf{X}_0$ (the problem then is three-dimensional rather than six-dimensional). In that case, (3) reduces to (1). If the observer is moving but the velocity vector is known, the position vector can be obtained from the first three rows on the left side of (3) (actually, any three rows) if the terms involving $v_1$, $v_2$, and $v_3$ are moved to the right side.

If the observations have different uncertainties, then the algorithm should minimize the weighted sum, $\mathcal{D}_w = \sum_i (w_i\delta_i)^2$, where $w_i$ is the dimensionless weight of observation $i$. The weight, $w_i = \sigma/\sigma_i$, is the ratio of the average uncertainty of all the observations, $\sigma$, to the uncertainty of the particular observation, $\sigma_i$. (Often it is desirable that $\sum w_i^2 = n$, so that $1/\sigma^2 = \frac{1}{n}\sum(1/\sigma_i^2)$.) The uncertainty of an observation is usually dominated by the angular measures that define the vector $\mathbf{d}_i$ for the observation (see section below on random errors). Including observational weights is accomplished simply by including the extra factor $w_i^2$ in each of the sums in (3).

## CURVATURE TERM

The third term in our motion model $\mathbf{X}(t) = \mathbf{X}(t_0) + \mathbf{V}_0 t + f(t)\mathbf{x}_0$ describes the curvature of the path in the direction $\mathbf{x}_0$, which, for a geocentric coordinate system and $f(t) < 0$, will be toward the center of the Earth. The term's value at the time of observation $i$ is $f_i = f(t_i)$; the term can then be written $\left(\frac{f_i}{X_0}\right)\mathbf{X}_0$ and we have assumed that $f_i/X_0$ is a known (dimensionless) quantity. For short tracks on the surface of the Earth, $f_i/X_0$ is small. For example, even for a 100-km track, $f_i = -0.8$ km, so $f_i/X_0 \approx 10^{-4}$.

In many cases, the curvature term may be unnecessary. It would be important for navigation applications on or near the surface of the Earth in which observations are collected over a track that may extend to some tens of kilometers or more and navigational accuracies of better than 100 m are expected. Generally these would be aircraft applications. It is used in place of an acceleration term in the solution, which would require three more unknowns (and at least two more observations) and which would, in many cases, be poorly determined because of its smallness compared to observational error.

For most purposes the magnitude of the term can be well represented by the parabolic approximation

$$ f_i = -\frac{1}{2}\frac{(vt_i)^2}{R} \quad \text{or} $$

$$ \frac{f_i}{X_0} = -\frac{1}{2}\frac{(vt_i)^2}{RX_0} \underbrace{= -\frac{1}{2}\left(\frac{vt_i}{X_0}\right)^2}_{\text{if } R=X_0} \tag{4} $$

where $R$ is the radius of curvature of the path, $v = |\mathbf{V}_0|$ is the speed of motion, and $vt_i \ll R$. The length $vt_i$ is the distance traveled from the reference point (where $t = 0$ and $\mathbf{X} = \mathbf{X}_0$) to the position of observation $i$, taken at time $t_i$. For an observer in a circular Earth orbit, $R = X_0$ and $v^2 = GM/X_0$, where $GM$ is the geocentric gravitational constant, but we will not consider the orbital case further here. For an observer on or near the surface of the Earth, a great-circle course is implied. For such an observer, if we consider the Earth to be a sphere, $R = X_0 = a + h$, where $a$ is the radius of the Earth and $h$ is the height above sea level. Note that some pre-solution estimate of speed is necessary for the evaluation of the term.

On the real, oblate Earth, things are a bit more complicated, because $R \neq X_0$, that is, the local radius of curvature is not the same as the local geocentric distance, and both vary from place to place. Formulas for radius of curvature and distance to the geocenter are given in any elementary geodesy text, for example, [12, 15, 16]. However, in most cases, the spherical-Earth approximation will work sufficiently well. For high-accuracy applications, or those where the observation track is extended, only very crude estimates of the observer's position, direction, and speed are needed to evaluate the term. The curvature term is discussed more fully in [14], which provides estimates of its sensitivity to assumed location and speed.

## PROPAGATION OF RANDOM ERRORS

As an application of least-squares, the algorithm represented by Equation (3) assumes that the observations are uncorrelated and that they have normally distributed random errors. Systematic errors are assumed to be insignificant. The effects of some common systematic errors are treated in the next section. This section discusses the origin and propagation of random errors of measurement.

The algorithm given above differs from most least-squares applications in two important ways. First, the quantity that is minimized in a sum-of-squares sense is a euclidean distance in 3-D space that is related to, but is not itself, a measured quantity for each observation. These distances ($\delta_i$) will have a statistical scatter that reflects not just the errors of measurement but also the errors in the predetermined coordinates of the objects observed. Second, the method does not rely on a linearization around an approximately known set of parameters. The solved-for parameters are the position and velocity vector components, not corrections to the components of assumed vectors. Yet, despite the fact that no conditional (observation) equations have been defined, most aspects of least-squares analysis still apply.

For example, as previously stated, the inverse of the 6×6 matrix in Equation (3), $A^{-1}$, is the unscaled covariance matrix of the solution. We can use it in the conventional way to obtain the formal uncertainties of the six solved-for parameters, $(x_1, x_2, x_3, v_1, v_2, v_3)$, and the parameter correlation matrix:

$$ \text{If} \quad A' = \left(\frac{\mathcal{D}}{2n-6}\right)A^{-1}, \quad \text{then} \quad \begin{cases} \sigma_i^2 = A'_{ii} \\ \sigma_{ij}^2 = A'_{ij} \\ c_{ij} = A'_{ij}/(\sigma_i\sigma_j) \end{cases} \tag{5} $$

where $\sigma_i^2$ is the formal variance of parameter $i$ ($i = 1$ to 6), $\sigma_{ij}^2$ is the formal covariance of parameters $i$ and $j$, and $c_{ij}$ is the correlation ($-1$ to $+1$) between parameters $i$ and $j$. We could, then, use the variances and covariances of $x_1$, $x_2$, and $x_3$ to form an error ellipsoid in 3-D space that represents the uncertainties in the solution for $\mathbf{X}_0$, or propagate the formal errors to any other position on the observer's track to see how the error ellipsoid changes with time.

The factor $\mathcal{D}/(2n-6)$ represents the variance of the least-squares fit, i.e., a measure of the scatter in the post-solution residuals. We have $\mathcal{D} = \sum_i \delta_i^2$, where each $\delta_i$ is the distance between the LOP of observation $i$ and the computed position of the observer at the same time. The quantity $2n - 6$ represents the number of degrees of freedom in the solution and reflects the fact that each of the $n$ observations is two-dimensional, i.e., it consists of two independent angular measurements. Each $\delta_i$ in the sum can be calculated using

$$ \delta_i = |\mathbf{d}_i \times (\mathbf{P}_i - \mathbf{X}_i)| \tag{6} $$

which is the minimum distance from point $\mathbf{X}_i$ to its associated LOP, $\mathbf{P}_i + r\mathbf{d}_i$. The symbols have the same meanings as in Equations (1) and (3), and $\mathbf{X}_i = \mathbf{X}_0\left(1+\frac{f_i}{X_0}\right) + \mathbf{V}_0 t_i$, with $\mathbf{X}_0$ and $\mathbf{V}_0$ taken from the solution. (Equation (6) is adopted from [17].)

The post-solution residuals can also be considered to be vector quantities:

$$ \delta_i = \mathbf{d}_i \times (\mathbf{P}_i - \mathbf{X}_i) \times \mathbf{d}_i \tag{7} $$

with the vector $\delta_i$ extending from the point $\mathbf{X}_i$ to the nearest point on its associated LOP. The length of the vector is $\delta_i$ (since $|\mathbf{d}_i| = 1$). Considered as a time series, the vectors $\delta_i$ contain all the information on the influence of the observations on the solution, with the effect of each observation proportional to $\delta_i^2$ (or, if weighted, $(w_i\delta_i)^2$).

Prior to a solution it is easy to obtain an estimate of its accuracy by considering, in general terms, the geometry of the LOPs. For this purpose, we assume that all the observations are of similar quality and
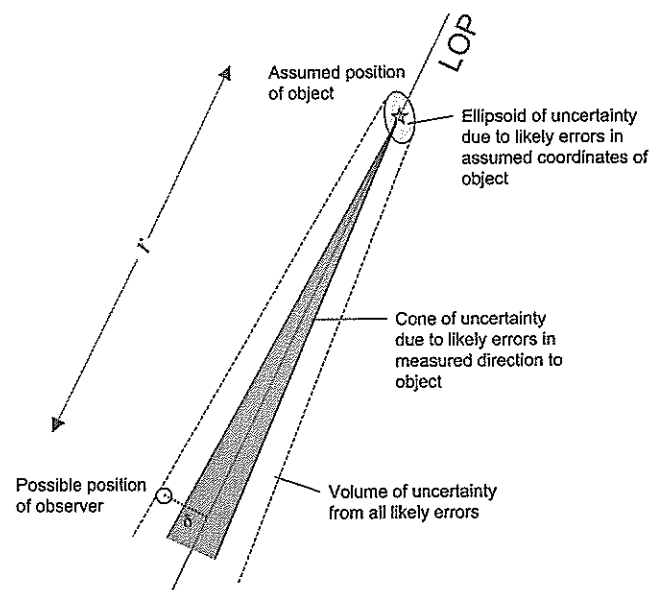
Fig. 3–Geometry of error propagation along a line of position. Statistically, the observer's position should lie within the LOP's volume of uncertainty.

are well distributed in direction and time, that is, that there is little or no geometric dilution of precision. As shown in Figure 2, each LOP is defined by both its "anchor" in 3-D space, a point at the assumed coordinates of the object observed, and its direction, defined by the observation itself. Given that the equation of the LOP is $\mathbf{X} = \mathbf{P} + r\mathbf{d}$ (where $r$ is a scalar of arbitrary value), the statistical uncertainties at a distance $r$ from the object are related by

$$\sigma_X^2 = \sigma_P^2 + r^2\sigma_d^2 \qquad (8)$$

where each $\sigma$ is the root-sum-square of the uncertainties in the respective vector components. Since $\mathbf{d}$ is always a unit vector, $\sigma_d$ represents an angular uncertainty in radians, which is developed below; we anticipate that it will be closely related to the centroiding error of the imaging system. Figure 3 represents a geometric interpretation of (8). The first term on the right of the equation represents the average radius of an ellipsoid of uncertainty around the assumed position of the observed object due to the likely errors in its coordinates. The $r$-term represents a cone of expanding uncertainty with its axis along $\mathbf{d}$, its apex at the assumed position of the object (where $r=0$), and its apex angle equal to $2\sigma_d$. The LOP could therefore plausibly be any line originating within the ellipsoid of uncertainty with a direction parallel to any line within the cone of uncertainty.

We expect the observer to be somewhere within, or not far outside of, each LOP's volume of uncertainty. So for observation $i$, we have $\delta_i \approx \sigma_X(r_i)$, for which we need at least a crude estimate of $r_i$, the

distance of the object from the observer. If the values of the $\delta_i$'s computed this way are similar, which would generally be the case if the distances to the observed objects were not too different, then a typical $\delta_i$, say $\bar{\delta}$, will be a predictor of the scatter in the post-fit residuals. That is, $\bar{\delta}^2$ should approximately equal the variance of the fit. We therefore have a simple way to anticipate the accuracy that can be obtained by various observing schemes.

The one remaining piece of unfinished business is determining the value of $\sigma_d$ to use in Equation (8). If the measurement of angles were absolute, that is, obtained from the pointing of the imaging system (say, from shaft encoders on the axes), then $\sigma_d$ would simply be the larger of the mechanical pointing resolution or the image resolution. However, such a system would require a transformation of the angular measurements from an instrumental system to a geodetic system before Equation (3) could be applied. Generally, that transformation is unknown. The advantage of differential measurements (i.e., nearby points measured with respect to more distant ones within a limited field of view) is that they avoid the problem of the unknown instrumental attitude. The orientation of the instrument need not even be measured.

For differential measurements, the geometry of how the observation vector is formed is shown in Figure 4. The figure shows the effect of finite imaging resolution, which creates an ambiguity in which vector to choose. That ambiguity defines the angular uncertainty of the observation, $\sigma_d$, used in Equation (8). The figure is based on the assumption that that the finite imaging resolution is the primary source of uncertainty and that the errors in the object coordinates are not the limiting factor. The geometry yields the result that $\sigma_d = \Delta\theta(\frac{1}{2} + \frac{r}{r'-r})$, where $\Delta\theta$ is the imaging resolution, and $r$ and $r'$ are the distances to the near and far objects, respectively (we assume that the far objects have some typical, or at least minimum, distance). We see that as $r' \to \infty$, $\sigma_d \to \Delta\theta/2$, so that very distant background objects are preferred. Note that in any case we require that the background objects be significantly behind those in the foreground so that the term $\frac{r}{r'-r}$ does not blow up. If a moving observer waits for a pre-selected foreground object to appear to line up with a pre-selected background object, the situation is similar. The diagram for this case is somewhat different but the resulting expression for $\sigma_d$ is the same.

## EFFECTS OF DEVIATIONS FROM THE IDEAL TRACK

Equation (3) is based on an observer trajectory that curves only toward the center of the Earth, that is, the path over ground is a great circle.
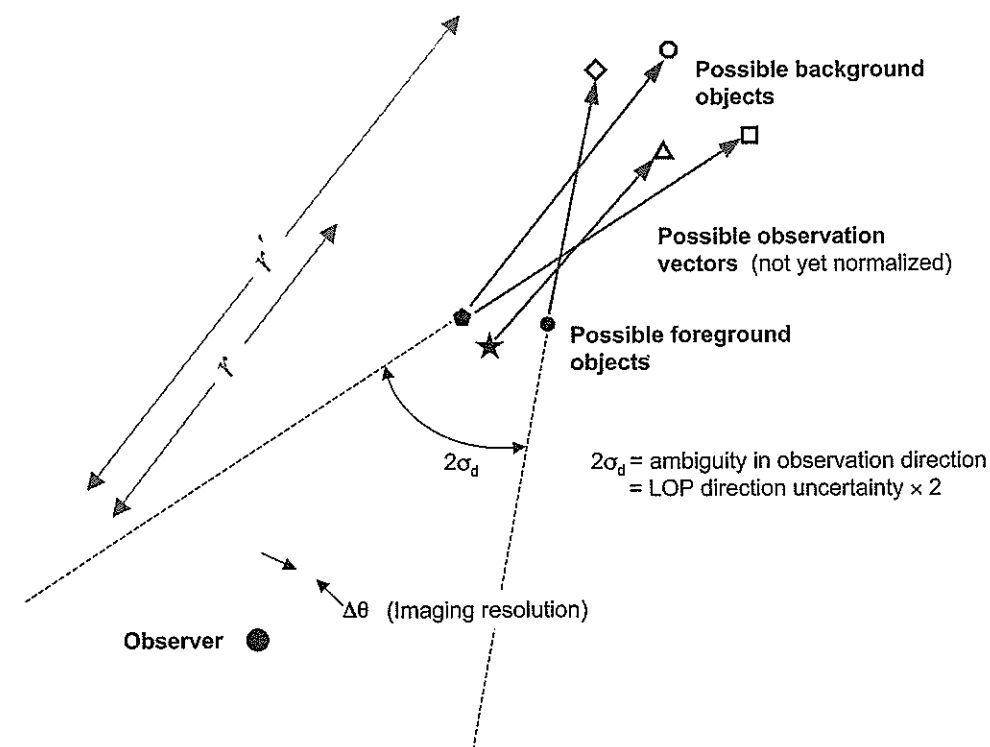


Fig. 4–Possible observation vectors for foreground objects viewed against background objects, at distances from the observer of $r$ and $r'$, respectively. (Not all possible vectors are shown.) The imaging system cannot distinguish among objects in the gray cone, defined by the image resolution $\Delta\theta$. The figure shows a spread of possible observation vector directions (= LOP directions) within an angle $2\sigma_d$.

Clearly, this ideal will seldom play out in practice, and it is important to evaluate the consequences of deviations from the modeled motion.

First, both ships and aircraft often follow rhumb lines rather than great circle routes. Over long distances, a great circle route may be approximated by a series of rhumb lines. A rhumb line (loxodrome; a track of constant azimuth) is a straight line on a Mercator map, but it generally has curvatures in two directions when viewed in a 3-D coordinate system. Curvature in the horizontal plane has not been accounted for in the development here. Rhumb lines diverge most rapidly from great circles for east-west tracks (except for latitudes within a few degrees of the equator, where the divergence is small in any case) with the effect being greater at higher latitudes. At 40 deg latitude, the maximum horizontal difference between a rhumb line and a great circle is 41 m over a 50 km track and 164 m over a 100 km track, if the end points are the same. Except for possible applications involving high-speed aircraft, then, the systematic error of following a constant heading rather than a great-circle route would not appear to be a major issue. Other systematic shifts in the vehicle's track are likely to be more important.

For example, it is worthwhile investigating how the algorithm responds to low-grade accelerations that might result from a systematic change in wind or current during the time period covered by the observations. For these cases, the results of [18] provide some insight. The appendix of that paper develops the general case of a least-squares fit of a linear motion model to position observations when the actual motion involves a weak acceleration. The paper provides expressions for the systematic errors of the solved-for parameters as well as for the statistics of the residuals. Here, the residuals we are interested in are the distances between the solution track and the true (accelerated) track, evaluated at the times of the observations. Of course, these residuals are only available for numerical test cases, and their statistical properties may differ from the observation residuals described by Equation (6). Although the type of observations and the form of the solution is different in [18] from that considered here, numerical tests verified that the geometry is similar enough to provide usable estimates of the magnitude of the effects. These tests indicated that Equation (3) generally produces smaller increases in the maximum residual than predicted by [18] but somewhat greater increases in

the RMS of the residuals, relative to a solution without acceleration included in the vehicle track.

For reasonable cases the solution adjusts itself such that the residuals do not increase dramatically when an acceleration is introduced. The aforementioned paper predicts that the maximum residual will increase by about $a\Delta t^2/12$, where $a$ is the acceleration and $\Delta t = t_n - t_1$ is the span of observation times. For example, a ship traveling at 50 km/h (27 kn) will cover 8.3 km in 10 minutes; a 100 km/h$^2$ acceleration will shift the track by 1.4 km over the same time. (This acceleration, approximately $1 \times 10^{-3}$ g, is equivalent to moving into a 9 kn current during that time.) Numerical simulations of this scenario (among others) were computed, both with and without acceleration, all with great-circle track solutions formed according to Equation (3) based on ten noisy artificial data points. In one typical case, the maximum residual increased by 0.20 km (from 0.29 to 0.49 km) when the acceleration was introduced. The above expression from [18] predicted an increase of 0.23 km. The RMS of the residuals increased by 36% (from 0.19 to 0.26 km); the predicted increase was 14%.

Although the past positions computed from the accelerated solution were only moderately degraded, relative to those from an unaccelerated solution, the solved-for velocity does not provide an accurate prediction of the future track, whether it is accelerated or not. For the above case, with acceleration included, the difference between the solved-for velocity (essentially, the average velocity over the 10-minute period of the observations) and the instantaneous velocity at either endpoint was 8.1 km/h (the prediction was 8.3 km/h), that is, a 17% error, with the error vector parallel to the direction of the acceleration. Overall, if the solution were used to extrapolate the observer's position 10 minutes beyond the span of observations, we should expect a systematic error of about 1.6 km if the future motion was unaccelerated and 3.0 km if the acceleration continued. On the other hand, if both the acceleration and the observations continue, a set of rolling solutions (i.e., using observations within a moving window of time) could provide the acceleration from the continuous change in velocity from one solution to the next.

We can construct approximate formulas for the applicability of the algorithm in the presence of acceleration, based on either of two criteria. We use the expressions in [18] that show that at the beginning and end of the observation interval, which spans time $\Delta t$, the solution's velocity will differ from the observer's instantaneous velocity by $a\Delta t/2$ and the systematic error in position there is $a\Delta t^2/12$. The uncertainty of the solution projected to time $t$ is $\sigma(t) = \sqrt{\sigma_x^2 + (\sigma_v(t - t_0))^2}$, where $\sigma_x$ and $\sigma_v$

are the formal uncertainties in position and velocity, respectively (their covariance is ignored here), and $t_0$ is the epoch chosen for the solution parameters, which we assume to be at the end of the observations. Then the expected position errors, $e$, at times $t_0$ and $t_0 + \Delta t$ are, respectively,

$$e(t_0) = \frac{1}{12}a\Delta t^2 + \sigma_x \quad \text{and}$$
$$e(t_0 + \Delta t) = \frac{7}{12}a\Delta t^2 + \sqrt{\sigma_x^2 + (\sigma_v\Delta t)^2} \quad (9)$$

In the latter case, we have assumed that the acceleration does not continue beyond the end of the observations; if the acceleration continues, the fraction $\frac{7}{12}$ would be replaced by $\frac{13}{12}$. If $e_{\max}$ is the maximum allowable navigation error, then using the above expressions, we find that as long as

$$a < 12\frac{(e_{\max} - \sigma_x)}{\Delta t^2} \quad \text{or}$$
$$a < m\frac{\left(e_{\max} - \sqrt{\sigma_x^2 + (\sigma_v\Delta t)^2}\right)}{\Delta t^2} \quad (10)$$

the solution will be acceptable. "Acceptable" means, in the first case, that the expected position error at the end of the observation interval (at $t_0$) will be less than $e_{\max}$, and in the second case that the solution could be projected another interval $\Delta t$ into the future (to $t_0 + \Delta t$) with error less than $e_{\max}$. In the latter expression, $m = 12/13$ if the acceleration continues and $m = 12/7$ if it does not. In the example referred to in the preceding paragraphs, $\sigma_x = 0.25$ km and $\sigma_v = 2.24$ km/h for the solution with acceleration, and $\Delta t = 1/6$ h. If we assume that the acceleration continues after the observations ($t > t_0$), so that $m = 12/13$, and we set $e_{\max} = 1$ km, then the acceleration $a$ would have to be less than 18 km/h$^2$ (equivalent to moving into a 1.7 kn current over 10 minutes) for the solution to be acceptable based on its predictive ability beyond the observations. But if only the positional accuracy at the end of the observation span were the criterion, the acceleration could be as high as 400 km/h$^2$, i.e., over 20 times greater, for the solution to be acceptable.

Of course, the real world is more complicated. In most cases we would have little information on the magnitude of any such acceleration, and it is unlikely to be constant for extended periods of time anyway. The actual track of the vehicle will in general be subject to both systematic and random-walk shifts due to changing wind or currents or steering or propulsion variations. The navigation solution described here, although computed for the specific instant $t_0$, really reflects a kind of average track of the vehicle during the observations. In that way it differs from near-instantaneous determinations of

position and velocity such as from GPS. The accuracy of dead-reckoning predictions based on a single navigation solution of either kind will vary widely depending on conditions. Although the Equation (3) algorithm has limited predictive ability when a constant acceleration is present, it would do well if the track variations were stochastic or nearly so and enough observations were used to provide an unbiased sample. Stochastic track variations have the same general effect on a solution as an increase in the random errors of observation.

## THE USE OF SATELLITE OBSERVATIONS

As was mentioned in the second section of this paper, a specific proposed application would use optical or near-infrared measurements of the angular positions of satellites observed against a star background. Such a system could provide a standalone backup against jamming of GPS signals, although likely of lesser accuracy. GPS satellites present point-like images (about 0.1 arcsecond across, less than the atmospheric "seeing" disk) in the visual magnitude range of 11–14, depending on the Sun-satellite-observer angle [19]. The main challenge in obtaining such observations is the large difference in the angular motions of the GPS satellites and the background stars, which can exceed 30 arcsec/s (0.5 deg/min) as seen from the surface of the Earth. Nevertheless, the satellites are observable in small telescopes with modern electronic sensors. Because the observed satellites are at finite distances, with geocentric coordinates known to a meter or better (readily available on the Internet) a straightforward triangulation method, such as the one presented in this paper, is feasible. Other satellites with accurately known orbits, e.g., geosynchronous communications satellites, or low-Earth-orbit (LEO) geodetic satellites, might also serve as observational targets.

Of course, the observer must know his position at least approximately to be able to plan observations. For GPS satellites, which are at a minimum height of about 20,000 km, the observer's position must be known only to within 175 km for a satellite to fall within a pre-pointed 1 deg field of view (angular error 0.5 deg). For LEO geodetic satellites, with typical heights of 1000 km, the observer's a priori position must be known to within 9 km. For cameras with apertures of about 20 cm, and charge-coupled device (CCD) sensors in the focal plane, exposure times would be less than a minute, often only a few seconds, depending on the satellite geometry. (The required exposure is thus less than the time needed for the satellite to cross a 1 deg star field.) The CCDs could work in either conventional "stare" mode or time-delay integration (TDI)

mode. In TDI mode, charge is moved across the sensor chip at a controlled rate that matches the angular motion of the object of interest, so that the object's image accumulates charge as it moves across the chip. A camera designed to observe GPS satellites would probably use both types of CCDs in the focal plane, one type for the satellite, the other for the stars. Image timing accurate to about a millisecond in UTC is required. Generally, GPS satellites would be night objects, but some daylight observations might be possible with near-infrared sensors. Successful daytime experimental observations of LEO satellites have been carried out with such sensors.

Each satellite observation would be expressed in some sort of "space fixed" celestial coordinate system while the satellite ephemeris position would most likely be expressed in a geodetic system that rotates with the Earth; a transformation of the observational data from the celestial to the terrestrial system will be required. In practice, there are two fundamental coordinate systems that are most appropriate for this problem: the International Terrestrial Reference System (ITRS) and the Geocentric Celestial Reference System (GCRS). The ITRS is a 3-D geocentric system that rotates with the Earth, so, loosely speaking, it is a "crust-fixed" system; more precisely, its axes have no net rotation with respect to the ensemble of ITRS defining stations. Geodetic positions in the ITRS coincide (within several cm) with positions measured with respect to the WGS-84 ellipsoid, e.g., from GPS. The ITRS is also referred to in GPS literature as the Earth-centered Earth-fixed (ECEF) system. The GCRS is the geocentric equivalent of the International Celestial Reference System (ICRS), which has its origin at the solar system barycenter and which is used for modern star catalogs and planetary ephemerides. The GCRS axes have no net rotation with respect to distant objects in the universe. The GCRS is a natural system for expressing the positions of stars as they would be seen by an observer on or near the Earth at a specific time.

Since both the ITRS and GCRS are geocentric systems, the transformation between them consists of a series of rotation matrices:

$$\mathbf{r}_{\text{GCRS}} = \text{B P N S W } \mathbf{r}_{\text{ITRS}} \quad (11)$$

where $\mathbf{r}_{\text{ITRS}}$ is a vector in the terrestrial system and $\mathbf{r}_{\text{GCRS}}$ is the corresponding vector in the celestial system. The matrices listed account for, from right to left, polar motion, sidereal time, nutation, precession, and a constant "frame bias." These coordinate systems and the transformations that link them are described more fully in [20] and there are several software packages available on the web for carrying out this transformation or its inverse. This

transformation forms the link between each satellite observation (right ascension and declination with respect to the GCRS) and the ephemeris position of the satellite at the time of the observation (X,Y,Z with respect to the ITRS). Actually, the ephemeris position of the satellite should be obtained for the time of observation minus the light-time to the GPS satellite ($\approx$0.07 s). The light-time calculation can be fairly crude and could be based on the distance of the satellite from the geocenter ($\approx$26,600 km) and its observed zenith angle; alternatively, an approximate observer location and the satellite ephemeris could be used. (An error of 750 km in the light travel distance results in only a 10 m error in the satellite's position.)

If the image centroiding errors are, say, 1-2 arcsec, then, using $\sigma_d = \Delta\theta/2 = 5$ $\mu$rad, $\sigma_P = 1$ m, and $r \approx 23,000$ km, the expected scatter in the triangulation residuals, using Equation (8), would be around 115 m. However, tracking a satellite over just a few minutes could provide a large number of independent observations, and the uncertainty of the position solution could conceivably be reduced to a few tens of meters. An advantage of using GPS satellites is that the constellation is designed to provide good ranging geometry (i.e., to minimize GDOP), so usually the observational geometry would also be favorable for the kind of triangulation described in this paper.

Unlike traditional celestial navigation where the observed stars are assumed to be infinitely distant, and triangulation is therefore not possible, the satellite scheme does not require any reference to the local vertical. This is important for moving observers, where a precise determination of the local vertical cannot be made using direct onboard ("lab") measurements, since the gravity and acceleration vectors are inseparable. (Inertial navigation systems can provide a computed estimate of the local vertical.) The horizon, which ideally defines an external plane orthogonal to the local vertical, is often not visible or accurately measurable. Even when clearly visible and sharply defined, the horizon is actually a warped circle, at the level of precision needed, due to direction-dependent low-level atmospheric refraction. The satellite scheme circumvents the local vertical or horizon problem; additionally, because it uses small-field measurements from an electronic image, there is no need for precise large-angle calibration. Thus, for moving observers that require a supplement or backup to ordinary radio-based GPS navigation, angular measurements of GPS satellites with respect to the stars have several fundamental advantages over traditional celestial navigation, even if the latter is automated.

Additionally, the satellites, like the stars, provide an absolute attitude reference. If the observations

used for the position and velocity solution can be expressed in instrumental coordinates, then we have two bases for each such vector: an external reference system (either the ITRS or the GCRS) and the instrumental reference system. That is the information needed to solve "Wahba's problem" [21], about which there is an extensive literature and software base, and determine the attitude of the instrument.

## NUMERICAL SIMULATIONS

A software package was created to test the mathematics presented in this paper and to explore the properties of the solutions. The software computes the track of a hypothetical vehicle across the surface of the Earth, given an initial date and time and values for latitude, longitude, course, and speed; either a great-circle or a rhumb-line track can be selected. This track is "truth." The user can specify a time span within which a selected number of artificial observations will be created. For each observation, the software identifies a target object, obtains its coordinates, and computes an observation vector, with the target coordinates and "observed" direction subject to random errors. The ensemble of observation times, target coordinates, and observation vectors is then sent to the routine that sets up and solves Equation (3). The solution yields the vehicle's position (at a pre-selected time) and velocity in geocentric rectangular coordinates, which can be transformed into latitude, longitude, height, course, speed, and rate of change of height. This allows the computation of a "solution track," which is compared to the "true track" for the span of time covered by the observations; the differences are sampled at the times of the observations. For simplicity, a spherical Earth with a radius of 6378.137 km was assumed for all the tests reported here. A computer script was written that allowed large numbers of solutions to be formed and compared for a given test track, using a Monte-Carlo-type scheme. Many different solution scenarios were tested this way.

In computing the artificial observations, the software attempts to spread the observation times more or less evenly across the specified time span (say, a half-hour), although the exact times chosen are random. For each time chosen, the software checks the elevation angle and azimuth of GPS satellites as they would appear from the vehicle at that time. Actual GPS positions are used, derived from NORAD two-line orbital elements propagated to the time of observation using SPACETRACK software [22]. Any satellite to be "observed" must be at least 30 deg above the horizon, and the software attempts to select a satellite that significantly

Table 1—Hypothetical True Track and Artificial Observations

| UTC Time | Distance km | Latitude deg | Longitude deg | Obs # | Sat ID | Altitude deg | Azimuth deg | Range km |
|---|---|---|---|---|---|---|---|---|
| 03:31:21 | −23.9 | +39.89 | −50.24 | 1 | PRN 06 | 32.3 | 146.1 | 22635 |
| 03:39:27 | −17.1 | +39.92 | −50.17 | 2 | PRN 01 | 84.9 | 264.9 | 20315 |
| 03:45:57 | −11.7 | +39.95 | −50.12 | 3 | PRN 30 | 40.8 | 49.6 | 21678 |
| 03:47:43 | −10.2 | +39.95 | −50.10 | 4 | PRN 14 | 54.1 | 150.6 | 21106 |
| 03:51:05 | −7.4 | +39.97 | −50.08 | 5 | PRN 01 | 83.1 | 208.0 | 20315 |
| 03:52:37 | −6.2 | +39.97 | −50.06 | 6 | PRN 31 | 67.0 | 334.5 | 20742 |
| 03:57:09 | −2.4 | +39.99 | −50.02 | 7 | PRN 29 | 42.0 | 90.0 | 21913 |
| 03:59:15 | −0.6 | +40.00 | −50.01 | 8 | PRN 01 | 79.6 | 191.8 | 20348 |
| 04:00:00 | 0.0 | +40.00 | −50.00 | | | | | |

differs in azimuth from those recently observed. (In a real-world application, satellite positions computed by SPACETRACK, based on two-line orbital elements, would not be nearly accurate enough for this purpose. GPS positions with errors of a meter or less would have to be obtained from International GPS Service data sets distributed daily on the IGS web site.)

Each observation vector — that is, the unit vector that defines the direction of the LOP — is computed from the difference between the GPS position and the vehicle position for the same instant, both expressed in an ITRF-like rectangular coordinate system that rotates with the Earth (i.e., an ECEF system). No attempt is made to simulate an actual observing system, such as a telescopic CCD camera, or to determine which stars the satellite would be seen against. Light-time is neglected, as are effects such as refraction and aberration that would be the same for the satellite and the background stars. However, each observation is modified by adding a random error in angle, in a random direction. The magnitudes of the angular errors are normally distributed with a standard deviation (in arcseconds) provided by the user. Weights are not assigned to the observations.

The satellite positions are also subject to random position errors. Just as for the observation errors, the user provides a standard deviation (in kilometers) for the satellite position errors, which are then normally distributed in each of three dimensions. (Real satellite position errors are generally higher in the along-track than cross-track directions.)

A few generalities about the solutions: When the user-selected observational errors (standard deviations) are set to zero, the solutions are for practical purposes exact for great-circle tracks of a few tens of kilometers long, as expected. That is, the latitude, longitude, course, and speed obtained from the solution's position and velocity vectors are essentially identical to those that describe the true track for the same instant. Along the solution track, the positional errors are less than 1 m compared to

the true track. As the time span, hence the distance, over which observations are obtained increases, the errors for such "perfect observation" test cases also gradually increase, due to the small errors in the curvature term described in [14]. Most of these solutions used the correct vehicle speed $v$ in the curvature term. However, even if $v$ has a relatively large error (say, 30%), it is only necessary to solve Equation (3) twice, using, the second time, the value of $v$ obtained from the velocity vector from the first solution. Tests showed that the second solution is essentially identical to a single solution with $v$ known exactly.

**Example:** A typical solution for a ship's rhumb-line track is shown in Tables 1, 2, and 3. The ship was hypothesized to be moving at a constant speed of 50 km/h (27 kn) along a course 60 deg from true North. On 2008 February 19 at 04:00 UTC, the ship's position was 50 deg West longitude, 40 deg North latitude. Eight artificial observations of various GPS satellites were computed for times distributed over the previous half-hour, corresponding to a 25-km track at the ship's speed. The standard deviation of the observational errors was set at 1 arcsec (5 $\mu$rad) and the standard deviation of the GPS coordinates was set at 5 m. Equation (8) predicts a scatter in the residuals of just over 100 m for this case, most of which is from the angular uncertainty of the observations. The solution was computed for 04:00 UTC. As with all solutions to (3), only three data elements were involved for each observation: the time, the observed satellite's direction vector, and the observed satellite's geocentric position vector. Both vectors were expressed in ITRF-like rectangular coordinates that rotate with the Earth. (In Table 1, the range to each satellite is shown for information only and was not used in the solution.) Note that three observations of PRN 01 were selected as it passed nearly overhead; although the observing geometry is similar in each case, they sample the ship's position at different times.

The solution parameters are given in Table 2. The top half of the table gives the position and velocity vectors expressed in geocentric rectangular

Table 2—Solution for Ship's Position and Velocity at 04:00 UTC

|  | X<br>km | Y<br>km | Z<br>km | $\dot{X}$<br>km/h | $\dot{Y}$<br>km/h | $\dot{Z}$<br>km/h |
|---|---|---|---|---|---|---|
| Solution | +3140.644 | −3742.714 | +4099.755 | +22.879 | +40.496 | +19.031 |
| Truth | +3140.619 | −3742.844 | +4099.787 | +22.841 | +40.144 | +19.151 |
| Difference | +0.025 | +0.131 | −0.032 | +0.038 | +0.352 | −0.120 |
| Formal Mean Error | 0.098 | 0.078 | 0.082 | 0.436 | 0.311 | 0.273 |

|  | Latitude<br>deg | Longitude<br>deg | Height<br>km | Course<br>deg | Speed<br>km/h | $\dot{h}$<br>km/h |
|---|---|---|---|---|---|---|
| Solution | +40.00026 | −49.99879 | −0.085 | 60.0814 | 50.254 | −0.264 |
| Truth | +40.00000 | −50.00000 | 0.000 | 60.0000 | 50.000 | 0.000 |
| Difference | +0.00026 | +0.00121 | −0.085 | +0.0814 | +0.254 | −0.264 |

Table 3—Post-Solution Residuals

| Obs # | Distance<br>km | $dR_T$<br>km | $dN_T$<br>km | $dE_T$<br>km | $dU_T$<br>km | $dR_L$<br>km | $dN_L$<br>km | $dE_L$<br>km | $dU_L$<br>km |
|---|---|---|---|---|---|---|---|---|---|
| 1 | −23.9 | 0.051 | −0.030 | −0.003 | +0.041 | 0.044 | +0.025 | −0.004 | +0.036 |
| 2 | −17.1 | 0.025 | −0.008 | +0.024 | +0.006 | 0.132 | −0.118 | −0.057 | −0.006 |
| 3 | −11.7 | 0.053 | +0.007 | +0.047 | −0.023 | 0.101 | +0.088 | −0.029 | −0.041 |
| 4 | −10.2 | 0.063 | +0.011 | +0.054 | −0.031 | 0.182 | +0.047 | +0.172 | −0.031 |
| 5 | −7.4 | 0.082 | +0.017 | +0.066 | −0.046 | 0.049 | −0.017 | +0.046 | +0.001 |
| 6 | −6.2 | 0.092 | +0.020 | +0.073 | −0.052 | 0.093 | +0.006 | −0.091 | −0.019 |
| 7 | −2.4 | 0.119 | +0.026 | +0.091 | −0.072 | 0.097 | +0.025 | −0.063 | +0.069 |
| 8 | −0.6 | 0.132 | +0.029 | +0.100 | −0.082 | 0.061 | −0.055 | +0.024 | −0.009 |
| RMS |  | 0.090 |  |  |  | 0.111 |  |  |  |

coordinates, directly from the solution. The lower half of the table converts that data to geodetic coordinates on the spherical Earth model used. The last column at lower right is the rate of change of height.

Table 3 shows the post-solution residuals for each observation. The residuals on the left side of the table indicate the distance between the solution track and the true track at the time of each observation; $dR_T$ is the total distance between tracks, while $dN_T$, $dE_T$, and $dU_T$ are the components of that distance in the topocentric directions North, East, and up. The run of $dR_T$ values indicates the overall position error of the solution. The residuals on the right side of the table are similar, but they indicate the distance between the solution track and the line of position defined by each observation. As expected, the line-of-position residuals, which are the basis for the solution, appear randomly distributed whereas the track residuals show systematic trends. It is the RMS of the line-of-position residuals that are predicted by (8). Note that the $dU_T$ track residuals show the effect of small, non-zero values for the height and height-rate parameters; no attempt was made to constrain the solution's track to the surface of the Earth. The $dN_T$ and $dE_T$ residuals include the rhumb-line versus great-circle errors, although they are small (<10 m) for this case.

One hundred solutions for the same hypothetical rhumb-line track were computed, each with either 6, 7, 8, or 9 observations spread over the same half-hour (25 solutions each). The median position error (distance $dR_T$) was 70 m, and 74% of the position errors were less than 100 m. The distribution of the position errors appeared Poisson-like, with only one error out of 750 samples over 300 m (387 m) and just 25 (3%) over 200 m. In these tests, there was only a very slight hint that the solutions with the greater number of observations were better overall than those with fewer; generally the solution-to-solution variations dominated the statistics. Other numerical tests indicated that significantly increasing the number of observations does have a measurable effect in reducing the track errors.

## CONCLUSION

A unique, closed-form algorithm has been presented that provides a 3-D navigational solution for position and velocity given a sequence of angles-only measurements. The algorithm includes a correction term for the curvature of the Earth, so that observations can be collected over extended tracks if necessary. The kind of measurements proposed for use with this algorithm are those in which the apparent positions of foreground objects are imaged and measured against background objects, and coordinates in some well-defined reference system (or systems) are known for both. This represents a large class of applications, which includes the observation of satellites with accurate ephemerides, such as GPS, observed against a star background.

Numerical simulations have shown the algorithm to be mathematically correct and the solutions robust, even when the number of observations is small. The solutions provide timely navigation information at a useful level of accuracy for satellite-observing scenarios that are realistic and based on current instrumentation capabilities and data availability.

The method described in this paper and one version of a physical navigation system that implements it are the subject of U.S. patent applications 12/552534 and 12/319651 (20090177398), respectively.

## REFERENCES

1. Kachmar, P. M. and Wood, L., "Space Navigation Applications," *NAVIGATION*, Vol. 42, No. 1, Spring 1995, pp. 187–234.
2. Woffinden, D. C., *On-Orbit Satellite Inspection: Navigation and $\Delta v$ Analysis*, M.S. Thesis, M.I.T., SSL #9–04, 2004.
3. Hagen, E. and Heyerdahl, E., "Navigation by Images," *Modeling, Identification, and Control*, Vol. 14, No. 3, 1993, pp. 133–143.
4. Hafskjold, B. H., Jalving, B., Hagen, P. E., and Gade, K., "Integrated Camera-Based Navigation," *The Journal of Navigation* (Royal Institute), Vol. 53, No. 2, 2000, pp. 237–245.
5. Pachter, M., Porter, A., and Polat, M., "INS-Aiding Using Bearings-Only Measurements of an Unknown Ground Object," *NAVIGATION*, Vol. 53, No. 1, Spring 2006, pp. 1–20.
6. Veth, M. J. and Raquet, J. F., "Aircraft Testing of an Optical Inertial Navigation System," Joint Navigation Conference 2006 (Joint Services Data Exchange).
7. Betke, M. and Gurvits, L., "Mobile Robot Localization Using Landmarks," *IEEE Transactions on Robotics and Automation*, Vol. 13, No. 2, 1997, pp. 251–263.
8. Bekris, K. E., Argyros, A. A., and Kavraki, L. E., "Angle-Based Methods for Mobile Robot Navigation: Reaching the Entire Plane," *Proceedings of the IEEE Conference on Robotics & Automation*, April 2004, pp. 2373–2378.
9. Briechle, K. and Hanebeck, U. D., "Localization of a Mobile Robot Using Relative Bearing Measurements," *IEEE Transactions on Robotics and Automation*, Vol. 20, No. 1, 2004, pp. 36–44.
10. Dickmanns, E. D., "An Integrated Approach to Feature Based Dynamic Vision," *Proceedings: CVPR '88*, the Computer Society Conference on Computer Vision and Pattern Recognition, June 5–9, 1988, Ann Arbor, Michigan, pp. 820–825.
11. Crassidis, J. L., Alonso, R., and Junkins, J. L., "Optimal Attitude and Position Determination from Line-of-Sight Measurements," *Journal of the Astronautical Sciences*, Vol. 48, Nos. 2–3, April–September 2000, pp. 391–408.
12. Bomford, G., *Geodesy*, 3rd Edition, Oxford: Clarendon, 1971.
13. United States Coast Guard *Light List*, Vol. II, Atlantic Coast, COMDTPUB P16502.2, Washington: Government Printing Office, 2010.
14. Kaplan, G. H., "A Closed Form Position and Velocity Solution for Angles-Only Navigation," 2008, http://gkaplan.us/content/nav_by_angles.pdf.
15. Hosmer, G. L., *Geodesy*, 2nd Edition, New York: Wiley, 1930.
16. Torge, W., *Geodesy*, 3rd Edition, Berlin: de Gruyter, 2001.
17. Hummel, J. A., *Vector Geometry*, Reading: Addison-Wesley, 1965.
18. Kaplan, G. H., and Makarov, V. V., "Astrometric Detection of Binary Companions and Planets: Acceleration of Proper Motion," *Astronomische Nachrichten*, Vol. 324, No. 5, 2003, pp. 419–424. (An expanded version of the appendices of the paper is available at http://gkaplan.us/content/curvpath.pdf.)
19. Fliegel, H. F., Warner, L. F., and Vrba, F. J., "Photometry of Global Positioning System Block II and IIA Satellites on Orbit," *Journal of Spacecraft and Rockets*, Vol. 38, No. 4, 2001, pp. 609–616.
20. Kaplan, G. H., *The IAU Resolutions on Astronomical Reference Systems, Time Scales, and Earth Rotation Models: Explanation and Implementation*, U.S. Naval Observatory Circular No. 179 ( Washington: U.S. Naval Observatory), 2005. (Available online at http://aa.usno.navy.mil/publications/docs/Circular_179.php.)
21. Wahba, G., "A Least Squares Estimate of Satellite Attitude," *SIAM Review*, Vol. 8, No. 3, 1966, pp. 384–386.
22. Vallado, D. A., Crawford, P., and Hujsak, R., "Revisiting Spacetrack Report #3," Technical Note AIAA 2006-6753, American Institute of Aeronautics and Astronautics, 2006.

# NAVIGATION

## JOURNAL OF THE INSTITUTE OF NAVIGATION

**Fall          2011**

**Volume 58   Number 3**